

# PROCEEDINGS OF SPIE

[SPIDigitalLibrary.org/conference-proceedings-of-spie](https://www.spiedigitallibrary.org/conference-proceedings-of-spie)

## Fast-scanning dispersion-adjustable reference delay for OCT using fiber Bragg gratings

Changhuei Yang, Siavash Yazdanfar, Joseph A. Izatt

Changhuei Yang, Siavash Yazdanfar, Joseph A. Izatt, "Fast-scanning dispersion-adjustable reference delay for OCT using fiber Bragg gratings," Proc. SPIE 5140, Optical Coherence Tomography and Coherence Techniques, (2 October 2003); doi: 10.1117/12.500987

**SPIE.**

Event: European Conferences on Biomedical Optics 2003, 2003, Munich, Germany

# Fast-scanning, dispersion-adjustable reference delay for OCT using fiber Bragg gratings.

Changhuei Yang, Siavash Yazdanfar<sup>\*</sup>, and Joseph A. Izatt

Department of Biomedical Engineering

Duke University, Durham, NC 27708

<sup>\*</sup>Massachusetts Institute of Technology, Cambridge, MA 02139

## Abstract

We report on the use of two matched linearly chirped fiber Bragg grating (FBG) in the reference arm of a Michelson interferometer as a means to achieve variable optical delay. We demonstrate that the properties of a linearly chirped FBG can be exploited to achieve millimeters of optical delay with physical stretches of the FBG on the order of tens of microns; this allows for optical delay line configurations that are easily driven by piezo-electric actuators.

## Keywords:

Fiber Bragg gratings, optical delay line, OCT, chromatic dispersion

Over the past decade, optical coherence tomography (OCT) has proven its applicability in numerous clinical settings [1-3]. As the center of gravity of OCT development shifts towards clinical applications, where clinicians with little optical experience routinely use OCT systems, the need for a maintenance free design becomes more compelling. An ideal design should dispel with the need for any bulk optical elements and the alignment that these demands. A close examination of a typical OCT system will reveal that most of these bulk optical elements are associated with the scanning optical reference delay line.

While earlier works have demonstrated that it is possible to create an optical fiber based rapidly scanning optical reference delay line by stretching a long optical fiber coiled around a piezo-electric actuator[4], the solution can be improved in two aspects. First, glass lacks a crystalline structure; long term usage of an optical fiber under net tension necessarily deforms the fiber and introduces unwanted optical path delay. Second, an OCT design based on such a delay line would still lack a means to correct for group velocity dispersion (GVD) variations in the target samples.

We report an alternative optical fiber based optical reference delay line that can potentially eliminate both shortcomings. This design is based on the use of chirped fiber Bragg gratings (FBG) [5]. Briefly, an FBG is a segment of optical fiber on which a periodic refractive index variation has been created along its length. When the wavelength of the light propagating in the fiber matches twice the etched period, a reflection resonance is achieved and the light is reflected. By chirping the period of index variation, it is possible to create a broadband reflector within the fiber. FBGs have been applied to create add-drop lines and GVD compensators in telecommunication.

In this manuscript, we present an all optical fiber based optical delay line based on the use of a matched pair of linearly chirped fiber Bragg gratings (FBGs) [5]. The pair compensates for each other's chromatic dispersion. By stretching or compressing one of the FBGs, it is possible to create an optical delay that is orders of magnitude greater than the

actual physical stretch. This phenomenon arises from the fact that the resonance reflection location for each wavelength on the FBG segment moves further down the segment when the FBG is stretched and the period spacings in the FBG are changed.

The shortness of the FBG segments ( $\sim 1\text{cm}$ ) makes it possible for the segment to be mounted directly on a piezoelectric stack. This allows the operation of the PZT under net zero tension condition. Furthermore, the shortness of the FBG segments does not require them to be coiled for operation.

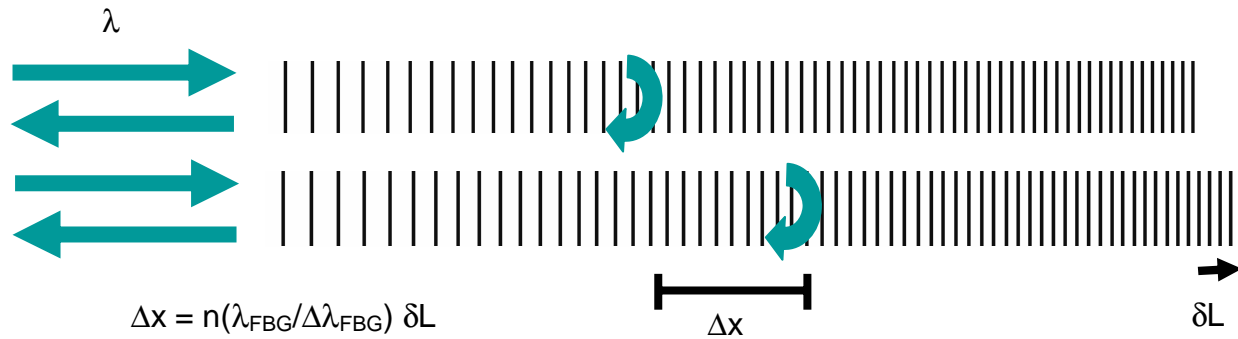


**Figure 1:** Light of a given wavelength will travel down a chirped FBG until it reaches the location where the refractive index variation period of the FBG matches with the wavelength. Light will then be resonantly from that location. Upon stretching the FBG, the refractive index variation period will increase and the light component will have to travel much further down the FBG before finding the correct variation period to resonantly reflect from.

We obtained a couple of matched linearly chirped FBG from BraggPhotonics. The units are centered at the wavelength of 1300nm and reflects strongly ( $>90\%$ ) over a bandwidth of 20nm. The units are fabricated through e-beam technology and are linearly chirped. They are each 1.0 cm long and have a refractive index of 1.47.

An input light beam will be reflected at different points along the FBG based on the wavelength of each component. Each monochromatic component (wavelength =  $\lambda$ ) is reflected at the resonance position,  $l$ , where:

$$\Lambda(l) = \frac{\lambda}{2n}, \quad (1)$$

$n$  is the fiber's refractive index. Upon stretching the FBG, the local fringe spacing expands. This in turn causes each wavelength component to be reflected at a point further down the FBG where the resonance condition is now met.

An optical delay line may be built by sending into one end of a linearly chirped FBG and channeling the reflection into an oppositely oriented identical FBG (see Fig 1a). The second FBG can be subjected to a stress/compression to alter its length by  $\delta L$ .

Mathematically, the fringe spacing,  $\Lambda_{1,2}$ , of the FBGs at location,  $l_{1,2}$ , along the fiber length can be expressed as:

$$\Lambda(l_1) = \Lambda_- + (\Lambda_+ - \Lambda_-) \frac{l_1}{L}, \quad (2a)$$

$$\Lambda(l_2) = \Lambda_+ + (\Lambda_- - \Lambda_+) \frac{l_2}{L} + \Lambda_+ \frac{\delta L}{L} \quad (2b)$$

where  $\Lambda_+$  and  $\Lambda_-$  are the maximum and minimum fringe periods at the ends of the FBGs without stress, and  $L$  is the total FBG length. Equation (2b) describes the fact that a stretch/compression of the FBG results in a change in the fringe period spacing. Light of a given wavelength will therefore resonantly reflect from a different location on the FBG when the FBG is stretched/compressed. The shift in reflection location can be much greater than the actual physical stretch.

By combining Eq. (1) and (2), we can derive the optical path delay for a given wavelength to be:

$$\begin{aligned} x_R(\lambda, \delta L) &= n(l_1(\lambda) + l_2(\lambda)) = nL + n \frac{\Lambda_+}{\Lambda_+ - \Lambda_-} \delta L \\ \Rightarrow \Delta x_R(\delta L) &= n \frac{\Lambda_+}{\Lambda_+ - \Lambda_-} \delta L, \\ &\approx n \frac{\lambda_{FBG}}{\Delta \lambda_{FBG}} \delta L \quad (\text{for } \lambda_{FBG} \gg \Delta \lambda_{FBG}) \end{aligned} \quad (3)$$

where  $\lambda_{FBG}$  is the FBG's center resonantly reflected wavelength and  $\Delta \lambda_{FBG}$  is the FBG's reflection optical bandwidth. The last equation is derived by noting that the fringe period spacing is proportional to the resonantly reflected wavelength from that location.

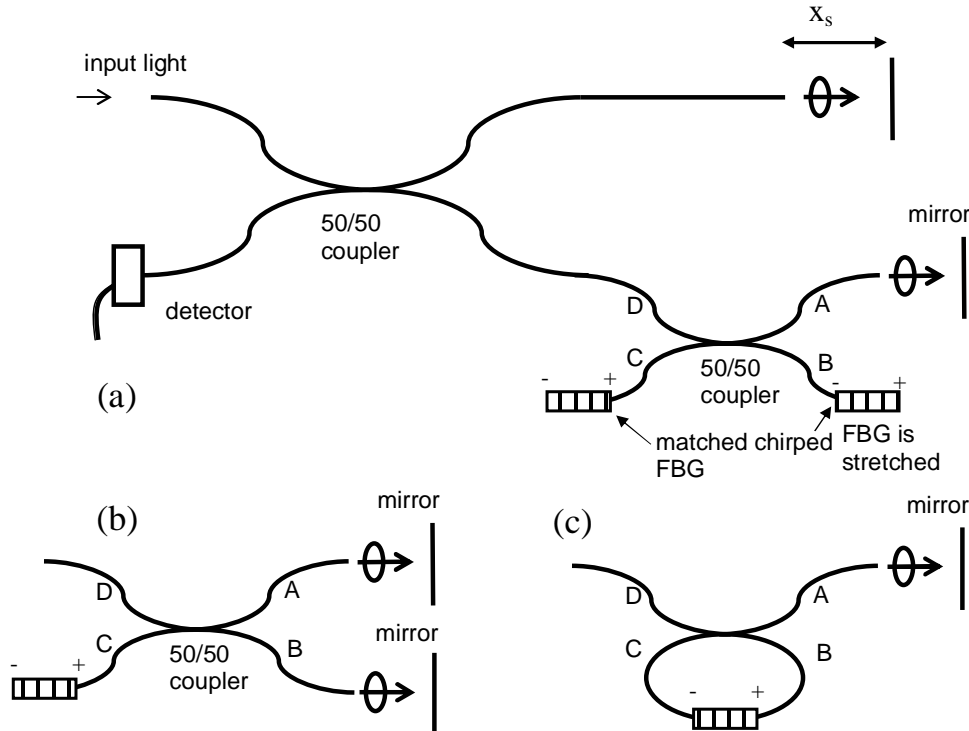


**Figure 2:** a) Experimental layout for matched FBG chromatic dispersion corrected variable optical delay line. + and - denote the orientation of each FBG. b) Experimental layout for a single FBG

configuration. c) Experimental layout where a single FBG is employed for chromatic dispersion correction.

There are two important notable points in the above equations. First, the optical delay is wavelength independent. This implies that this configuration will not introduce any dispersion on the light beam. In other words, even though a single chirped FBG is chromatically dispersive, the dispersion can be corrected by using two oppositely oriented FBG. Furthermore, this correction is unchanged even when one of the FBG is stretched. The second important point to note is that, as  $\Delta\lambda_{FBG}$  is typically much smaller than  $\lambda_{FBG}$ , the optical delay change due to the stretching of the FBG is much greater than the actual physical stretch.

These two points mean that we can build a dispersion free variable length optical delay line that can be actuated with a physical stretch that is much smaller than the optical delay change induced.

To verify that the above described geometry do indeed lead to neutralization of the FBG dispersion and enable the construction of a variable optical delay line, we constructed an experimental setup shown in Fig. 2a. An Optospeed superluminescent diode SLED1300D of center wavelength 1300 nm, power 20mW and FWHM spectral bandwidth of 31nm, was used as the light source. A scanning mirror mounted on a galvo is placed in one arm of the interferometer, while a pair of Bragg Photonics chirped FBG is used in the other arm of the interferometer. Light components traveling in the path D to C to B to A to D and the path D to A to B to C to D will be appropriately dispersion compensate. The other possible light trajectories ( $\sim 75\%$  of the light) lead to chromatically dispersed light components. However, by judicious choice of interferometer arm lengths and fiber lengths in all arms, these components will not result in interference signals that coincide with the interference from the two above mentioned trajectory. The resulting interference signal detected while the mirror scans is given by:

$$\begin{aligned}
 I_{S,R}(x_S) &= 2 \int_0^{\infty} S(\lambda) \sqrt{B(\lambda)} \operatorname{Re} \left( e^{-i2k\Delta x_S} e^{i2k\Delta x_R(\delta L)} \right) dk \\
 &\approx 2 \sqrt{I_R I_S} \cos[2k_o(\Delta x_R(\delta L) - \Delta x_S)] \operatorname{sinc} \left[ \frac{2\pi\Delta\lambda_{FBG}}{\lambda_{FBG}^2} (\Delta x_R(\delta L) - \Delta x_S) \right] \\
 &= 2 \sqrt{I_R I_S} \cos \left[ 2k_o \left( n \frac{\lambda_{FBG}}{\Delta\lambda_{FBG}} \delta L - \Delta x_S \right) \right] \operatorname{sinc} \left[ \frac{2\pi\Delta\lambda_{FBG}}{\lambda_{FBG}^2} \left( n \frac{\lambda_{FBG}}{\Delta\lambda_{FBG}} \delta L - \Delta x_S \right) \right]
 \end{aligned} \tag{3}$$

where  $S(\lambda)$  is the spectral profile of the light source,  $B(\lambda)$  is the reflection spectral profile of the FBG. The approximation is arrived at by noting that  $S(\lambda)$  is significantly wider than  $B(\lambda)$  and that  $B(\lambda)$  ( $\Delta\lambda_{FBG} = 20\text{nm}$ ) is sufficiently spectrally flat. The same interference signal prediction can be attained by replacing the FBG pair with mirrors and using a light source with spectral profile of  $B(\lambda)$ .

To compare, we also recorded the signal traces with other FBG configurations shown in Fig. 2b and 2c. The three signal traces can be found in Fig. 3. Not surprisingly, the detected signal trace when a single FBG was used (Fig. 3, top trace) shows dispersion artifacts. The

interference signal is significant over an optical path length of 1.5 cm – the optical path length of the FBG. This observation is consistent with the expectation that light is spectrally dispersed by the FBG with each wavelength component reflected by different location along the length of the FBG. The matched FBG configuration shows a significantly less dispersion artifact but does not match with theoretical prediction. The interference signal envelop has a FWHM value of 317  $\mu\text{m}$  while the theoretical prediction is 52  $\mu\text{m}$ . There are also significant ringing artifacts in the signal. We believe that these imperfections are due to the small mismatch of the two FBGs. This conjecture is supported by the experiment where a single FBG fulfills both roles of the two FBG in the original experiment (Fig. 2b). In such an experiment, we observed a signal envelop with FWHM value of 69  $\mu\text{m}$  (about 33% wider than the theoretical prediction). The signal is sharper and cleaner.

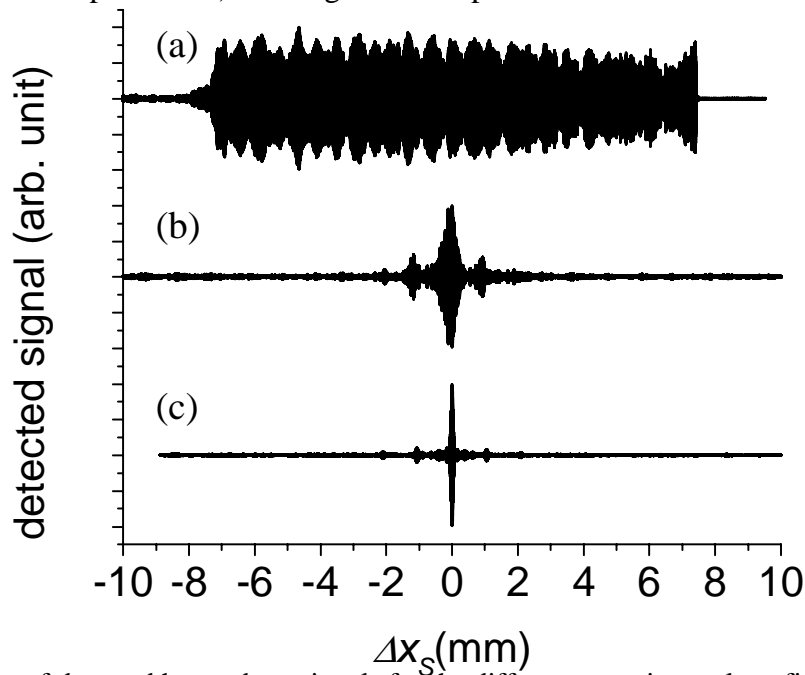


**Figure 3:** Plots of detected heterodyne signals for the different experimental configurations shown in Fig. 1. a) detected signal for configuration in Fig. 2b. b) detected signal for configuration in Fig. 2a. c) detected signal for configuration in Fig. 2c.

We then tested the optical path delay amplification effect of the original configuration. The predicted path amplification is given by:

$$\frac{\Delta x_R(\delta L)}{\delta L} = n \frac{\lambda_{FBG}}{\Delta \lambda_{FBG}} \quad (4)$$

One of the FBGs was progressively stretch by a PZT while the location of the interference maxima is monitored via the mirror displacement  $\Delta x_s$ . A total stretch of 33  $\mu\text{m}$  was achieved and the final observed optical delay shift was 3495  $\mu\text{m}$ . The optical path delay change is plotted in Fig. 4. The observed amplification factor of 106 agrees well with the predicted amplification of 96.

As we have demonstrated, FBG pair based arrangement can be used to create amplified variable optical delay lines. Our experiments highlighted the several technology improvements required for successful implementation. First, the method depends critically on

the match of the two FBGs used. This requirement seeks fabrication solution that is capable of high fabrication tolerance or fabrication process that is capable of fabricating two FBGs in the same fabrication run. This technological requirement appears attainable with the maturation of FBG fabrication techniques. The second desired improvement involves the increase of FBG reflection bandwidth. For OCT applications, a reflection bandwidth of more than 50 nm at the operating wavelength of 1.3  $\mu\text{m}$  is very desirable in order to allow sufficient reflection of light from a low coherence light source. From Eq. (4), we can see that this reduces the amplification factor to 40. Given the stress breakage limit of a typical optical fiber is a fractional length change of about  $3 \times 10^{-3}$ , this implies that we need an FBG of length 2.5 cm in order to attain a variable optical translation of 3 mm. This is an achievable objective as e-beam technologies can be used to make FBGs as long as 10 cm. As a final consideration, we would like to note that the total processed light fraction of this present system is low; a maximum of 25% of the input light will be processed. This is mostly due to the use of a fiber coupler in this initial demonstration. The processed fraction can be significantly improved through the use of optical circulators in place of the fiber coupler.

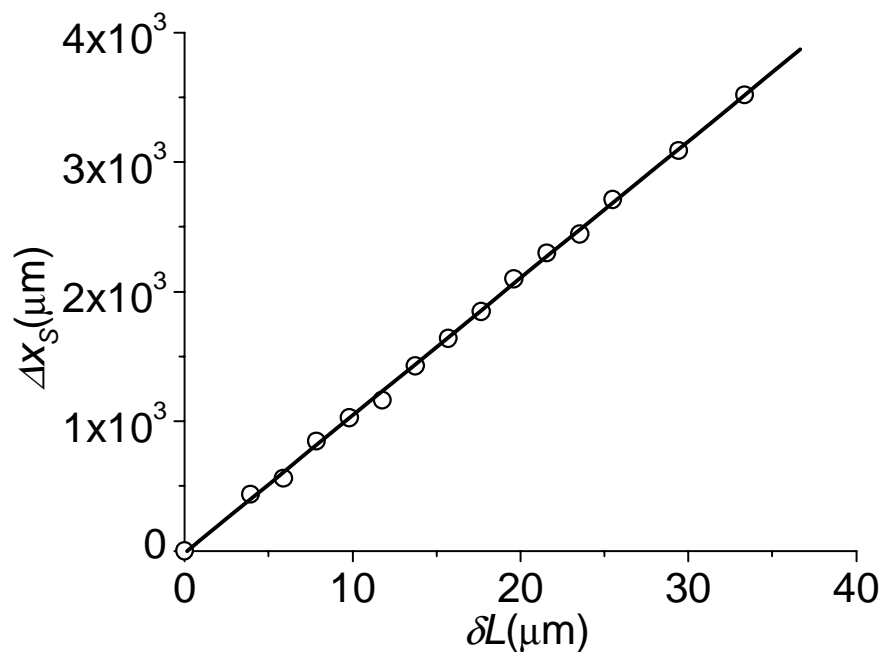


**Figure 4:** Plot of the optical delay ( $\Delta x_s$ ) induced by a physical stretch ( $\delta L$ ) of one of the FBGs for the experimental configuration depicted in Fig. 2a.

In conclusion, we demonstrated that a matched pair of linearly chirped FBG can be used to construct a novel optical delay line that is capable of large optical delay change (3.5 mm) actuated by small physical stretch/compression (33  $\mu\text{m}$ ). This new technique opens up the possibility for making very compact and low maintenance variable optical delay line. The main practical technological obstacle lies in high precision fabrication of closely matched pairs of FBGs such that their chromatic dispersion cancels out.

## Bibliography

1. Hee, M.R., et al., *Optical Coherence Tomography of the Human Retina*. Archives of Ophthalmology, 1995. **113**(3): p. 325-332.
2. Puliafito, C.A., et al., *Imaging of Macular Diseases with Optical Coherence Tomography*. Ophthalmology, 1995. **102**(2): p. 217-229.
3. Yazdanfar, S., A.M. Rollins, and J.A. Izatt, *Imaging and velocimetry of the human retinal circulation with color Doppler optical coherence tomography*. Optics Letters, 2000. **25**(19): p. 1448-1450.
4. Tearney, G.J., et al., *Rapid acquisition of in vivo biological images by use of optical coherence tomography*. Optics Letters, 1996. **21**(17): p. 1408-1410.
5. Ouellette, F., *Dispersion cancellation using linearly chirped Bragg grating in optical waveguides*. Optics Letters, 1987. **12**(7): p. 847.